Evaluation of the Design Parameters for Wireless Power Transfer System Applied in Electrical Vehicles

Abdulhamid B. Elganzory[1], Fathy R. Emam[1], Muhammed E. Abdulmoaty[1], Muhammed S. Ezzat[1], and Nagy I. Elkalashy[2*]

[1]Bachelor Student, Academic Year 2023/2024, Electrical Power and Machines Engineering Program, Electrical Engineering Department, Faculty of Engineering, Menoufia University, Shebin Elkom, 32511, Egypt.
[2]Team Supervisor, Electrical Engineering Department, Faculty of Engineering, Menoufia University, Shebin Elkom, 32511, Egypt.
(Corresponding author: nagy.elkalashy@sh-eng.menofia.edu.eg)

ABSTRACT

Wireless charging of electrical vehicles is essential as a preliminary stage for the dynamic charging of moving vehicles. It gives the vehicles the possibility to increase their driving range and decrease their battery size, which are the main problems of electrical vehicles. In this paper, the design prototype parameters of a wireless power transfer (WPT) system dependent on the inductive coupling power transfer mechanism are evaluated. The prototype of the wireless charging system has been designed using two circular coils arrangement. Using the COMSOL program, the physical implementation of the wireless transfer power system is studied. To efficiently correlate the output and input powers, the frequency and number of turns of the coils are varied and the results are evaluated to attain their optimum values that produce the highest efficiency. Based on the highest efficiency, the WPT system parameters have been selected. Finally, the developed prototype was experimentally implemented to verify the performance, though the desired frequency could not be acquired.

Keywords: *COMSOL Representation; Geometry Configuration; Magnetic Coupling; Multi-Level Inverter.*

1. Introduction

The electrical vehicle is one that operates on an electric motor, instead of an internal combustion engine generating power by burning a mix of fuel and air. The electrical vehicle stores the electricity in rechargeable large traction batteries to power the electric motor [1-3]. The electrical vehicle must be plugged into a wall outlet or charging equipment which is called electrical vehicle supply equipment.

The electrical vehicles have recently participated in combating climate change across the globe by helping to cut down emissions as electrical vehicles do not emit polluting gasses into the atmosphere [4]. Less noise pollution as the noise level while operating electrical vehicles is much lower than that of petrol or diesel engine-powered cars. It reduces dependence on fossil fuels. The electrical vehicles accelerate faster than cars with traditional fuel engines, so they feel lighter to drive. They are highly efficient as the efficiency of an electric motor is nearly 90%.

Incorporating wireless power transfer (WPT) systems into electrical vehicles has technical gains such as

avoiding electrical sparks as well as cable loss. From the system implementation point of view, there are two concepts of wireless charging that they are static and dynamic wireless charging systems [1-4]. The static one is to charge the battery of the electrical vehicle when it is turned off, while the dynamic one is to dynamically charge the battery of the electrical vehicle while it is moving. The main advantage of the dynamic wireless charging system is achieving a fully charged battery in accordance with reducing battery dependence. The reduced requirement of battery dependence enhances the expenses of the end users and the electrical vehicles infiltration [4-7].

The electrical vehicle wireless charging system consists of the primary and the secondary transmitting coils. The primary transmitting coil is supplied from an inverter to transfer the power at a high-frequency coupling. The inverter is used to modulate the AC power at high frequencies. To reduce the effect of the high-frequency magnetic coupling, the primary circuit contains a compensation element in the form of a capacitance effect. The secondary receiving coil as a

pickup coil is connected to the secondary compensation capacitor to reduce the high-frequency voltage drop for performing the power transfer system in the resonant state. The precise resonant WPT network enhances the power transfer capability. Also, on the secondary side, there is the DC-DC converter after rectifying the high-frequency power current to manage the battery charging energy. Therefore, the management system is used to control the wirelessly transferred during the charging state of the battery as well as its discharging state to provide the vehicle with the energy associated with the monitoring system [7-10].

The capacitive-based WPT system can also transfer power at high frequencies [7-9]. The capacitive power transfer system has the advantage of being unaffected by the surrounding metals. On the other hand, the inductive is influenced by the eddy currents that are increased at the high frequencies. However, the energy transferring rate of the capacitive type is lower than the inductive one, so the capacitive type can be used for wireless transferring power through small distances to be active at no resonance state.

In the literature, there are several geometry configurations of the coils, ranges of frequency, coil-rated parameters, and efficiencies [4,11-13]. That's the motivation to know the effect of varying those parameters. The objective of this study is to evaluate the different WPT systems and design a suitable one to charge the electrical vehicle and develop its accuracy. For that, the presented study is based on inductive coupling power transfer and introduces the evaluation of two designs of WPT system and with the theoretical results to determine the efficiency with gap variation to select the optimum design.

2. Aim and Research Significance
Figure (1) shows the scheme of the wireless charging system for the electrical vehicle. The most common distance for the application of a WTP is considered something like 5 cm [4]. May this distance be small for electrical vehicle design, so this distance is evaluated for a range of up to 20 cm. The wireless transferring power target of the prototype under study is up to 5 kW. The study is to evaluate the efficiency of gap distancing at different frequency ranges from 1 kHz up to 100 kHz.

To get the optimum design for the WPT system, COMSOL software simulation was used, then the results were exported to the MATLAB field to calculate the efficiency as shown in the flowchart depicted in Figure (2). The system which has the best efficiency is the one chosen to be implemented.
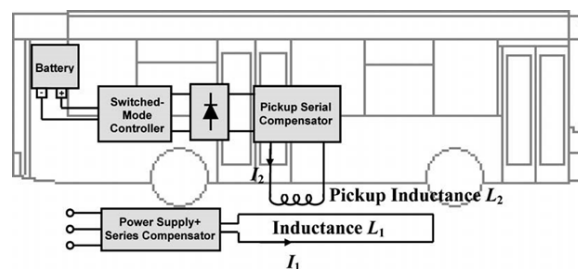

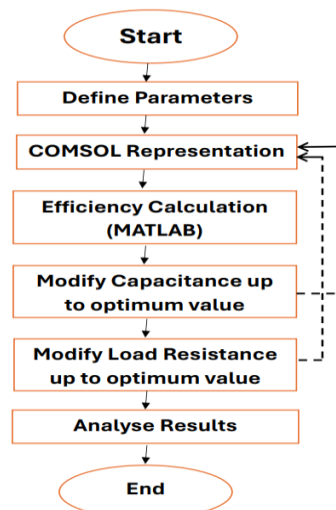Figure 1- Scheme of the ICPT battery charger [4].

Figure 2- Flowchart for the optimal design.

The utilized finite element program in this study is the COMSOL Multiphysics software. This software depends on solving the partial differential equations of several physics. Accordingly, it is appropriate for the engineering of electric, magnetic, mechanical, chemical, etc. sciences [14-16]. This can be applied individually and intermutually that enhance the study in the integrated form.

As the study is focused on efficiency evaluation, the coil performance is evaluated at different design parameters such as the capacitances, coupling frequency, and loadings that are considered by varying load resistance. The system is simulated using the COMSOL program first, where the used design is implemented using the 2D axis symmetry system to construct coils. This 2D implementation concept is considered to reduce the loading computation time of the computer solution. Accordingly, utilizing computers of high specification can be avoided. Then, the results are exported from the COMSOL to MATLAB with a sweep capacitance range keeping load resistance and frequency constant. The record results are exported to the Excel sheet to find the highest value of efficiency to select the optimum capacitance. Then at this assigned optimum

capacitance, this procedure is repeated, however for the load resistance to estimate the optimum loading.

As shown in Figure (2), the process starts with defining the parameters of the system, which include the number of turns per coil (N), frequency range (F), capacitance range for C1 and C2, load resistance (R), and material properties. The 2D axis symmetry system is utilized to construct the coils in COMSOL software. The number of 38 circles representing 19 turns for each coil with an inner radius (Rin) of 144.5 mm and a turning radius (r) of 2.5 mm, increasing by 4 mm for each circle are constructed. The air gap length between the coils is 20 cm. The material used for the conductor is copper and for the surrounding area is air. The upper circles represent coil 1, and the lower circles represent coil 2. The surrounding area is insulated for accurate calculations. The system parameter data are exported from COMSOL to the MATLAB script to evaluate the system transferring power efficiency. The capacitances are varied (C1 and C2) while keeping the load resistance (R) constant at 100 ohms and frequency (F) at 50 kHz. This frequency value and load value are as initial values. Then, the efficiency is calculated for each value of capacitance and finally, the result is recorded in an Excel sheet. From the system efficiency evaluation using the MATLAB script, the capacitance values corresponding to the highest efficiency are identified and hence the optimal capacitance for C1 and C2 can be determined. Then in the COMSOL field, the capacitances remained constant at the optimized value while varying the load resistance (R) along the specified range (20, 50, 80, 110, 140, 170, 200 Ω). Once again, the data are exported to MATLAB and the efficiency is evaluated for each value of the load resistance. Using the corresponding results recorded in an Excel sheet and uploaded to the MATLAB script, the load resistance value corresponding to the highest efficiency is identified and hence the optimal load can be determined. The process is repeated with different parameters to reach the optimized WPT model.

3. COMSOL Multiphysics Representation

3.1 Drawing the Inductive Coils

As aforementioned, the COMSOL 2D axis symmetry system is chosen for performing the parameter assessment of the wireless charging system. As in Figure (3.a), it shows the system construction on the 2D axis system. Starting to draw the receiving coil (19 turns) and the transmitting one (19 turns) using 38 circles, each circle represents a turn for one of these two coils as shown in the Model Builder. The distance between two coils (Air Gap) is 20cm. Figure (3.b) shows the two coils in the corresponding 3D.
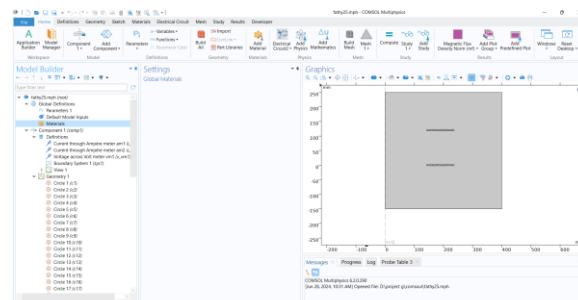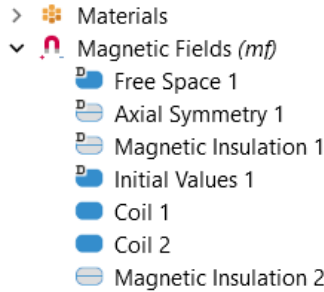

a. 2D axis symmetry system.
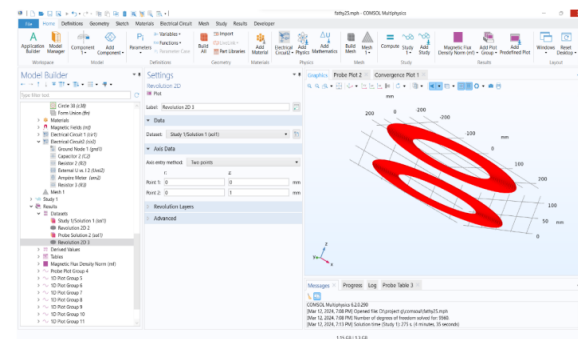
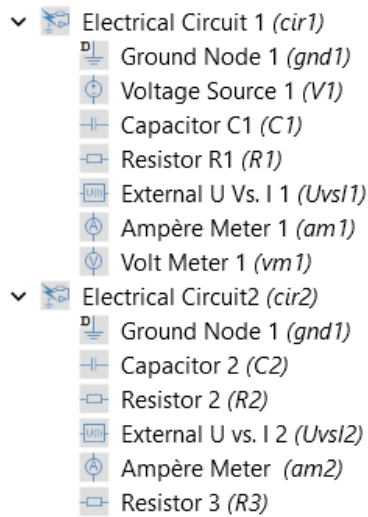b. The corresponding 3D.
Figure 3- COMSOL representation.

3.2. Magnetic Fields List

For the coils 1 and 2 construction, the upper circles are labeled as coil 1 and the lower circles are labeled as coil 2. Figure (4.a) shows the magnetic field list, which includes the two coils. For magnetic insulation, the area surrounding the wireless transferring system is defined, and its voltage equal to zero as a reference. For the electric circuit, which is shown in Figure (4.b), the electrical circuit is represented in the program by adding each element with a start and end number. By starting with the ground node which takes the number zero, then adding a voltage source with a start number of zero and an end number of 1. Then, add the first capacitor with a start number of 1 and an end number of 2. Then, complete all the elements in the same way as depicted in Figure (4.c). The two coils are represented by the two external elements. Therefore, the coil is taken and drawn with its material and its number of turns to include its bilateral interaction. Figure (4.c) shows the two electrical circuits that represent the primary and secondary coils for the application under study of the WPT system. May the stray capacitance affect the design parameters of the WPT system. However, the involved capacitances in the system to attain the resonance performance can be the dominant control of the capacitive effect. In the simulated system, the stray capacitances are included as the COMSOL program is used to implement the physical structure of the system. Furthermore, there
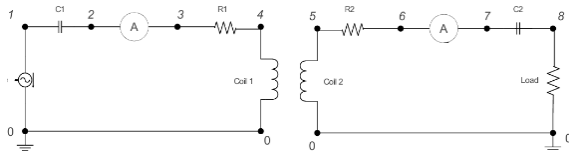
are challenges to implementing the battery and its drive system using the COMSOL software. Accordingly, the battery charging system is not involved in this study and it is replaced by the resistor. Similarly, it is considered experimentally.

> ⚏ Materials
∨ ⚏ Magnetic Fields (mf)
  ⚏ Free Space 1
  ⚏ Axial Symmetry 1
  ⚏ Magnetic Insulation 1
  ⚏ Initial Values 1
  ⚏ Coil 1
  ⚏ Coil 2
  ⚏ Magnetic Insulation 2

a. Magnetic fields list.

∨ ⚏ Electrical Circuit 1 (cir1)
  ⚏ Ground Node 1 (gnd1)
  ⚏ Voltage Source 1 (V1)
  ⚏ Capacitor C1 (C1)
  ⚏ Resistor R1 (R1)
  ⚏ External U Vs. I 1 (Uvsl1)
  ⚏ Ampère Meter 1 (am1)
  ⚏ Volt Meter 1 (vm1)
∨ ⚏ Electrical Circuit2 (cir2)
  ⚏ Ground Node 1 (gnd1)
  ⚏ Capacitor 2 (C2)
  ⚏ Resistor 2 (R2)
  ⚏ External U vs. I 2 (Uvsl2)
  ⚏ Ampère Meter (am2)
  ⚏ Resistor 3 (R3)

b. Electrical circuit list.

c. Electrical circuit.

Figure 4- Magnetic and Electric representation in the COMSOL field.

3.3. Numerical Calculation of the Efficiency

The MATLAB script is loaded by the data recorded in the Excel sheet that is exported from COMSOL, which represents an array of four columns. The first column includes the time values, the second one includes the values of the current at the transmitter, the third one includes the values of the current at the receiver, and

the fourth includes values of the voltage at the transmitter. The mean output power is calculated by:

$$P_o = \frac{\sum_0^n (I_o^2 R_L)}{n} \tag{1}$$

where, I_o represents the current at the receiver. Each value at the column of the current at the receiver is squared and multiplied by each value at the column of the load resistance, then summation is calculated to all values and divided by their number to get the mean value. The input power is calculated by:

$$P_i = \frac{\sum_0^n V . I_i)}{n} \tag{2}$$

where, I_i represents the current at the transmitter. Each value at the column of the current at the transmitter is multiplied by each value at the column of the voltage at the transmitter, then summation is done to all values and divided by their number to get the mean value.

## 4. Results and Evaluation.

4.1. Simulation Results

The results shown in Figure (5.a) are for the system efficiency evaluation over the system capacitances while keeping the loading resistance (R) constant at 100 Ω and the system frequency (F) at 50 kHz. From the results in this figure, the best capacitances of the primary and secondary sides are C1=C2=1.46E-07 F, in which the highest efficiency is found at 54%. The results shown in Figure (5.b) are to evaluate the efficiency at these selected capacitances and to estimate the loading of the highest efficiency under these circumstances. From the results in Figure (5.b), the highest efficiency is attained at loading R = 20 Ω, and the best efficiency is 68%.

By changing the system frequency to 60 kHz, and repeating the same steps as done for the evaluation at the frequency of 50 kHz, the results are reported in Figure (6). The results show that the best capacitance is at C1=C2=1.46E-07 F, in which the best efficiency is found 53% as depicted in Figure (6.a). Using this capacitances value, the results of load resistance at frequency 60 kHz are depicted in Figure (6.b). The results show that the best efficiency is attained at loading 50 Ω that the best efficiency is found at 62%.

The results shown in Figure (7) are for the wireless power transferring at a frequency of 85 kHz. From the curve in Figure (7.a), the best capacitance of the primary and secondary is C1=C2=1.46E-08 F, which has the best efficiency of 59%. Using this value of the capacitances, the results in Figure (7.b) are obtained that the best efficiency is at the loading in the range of 65 to 85 Ω, and the best transferring power efficiency is attained at 63%.
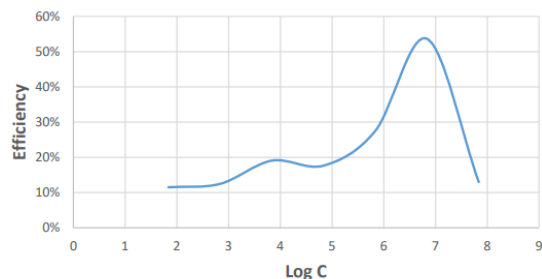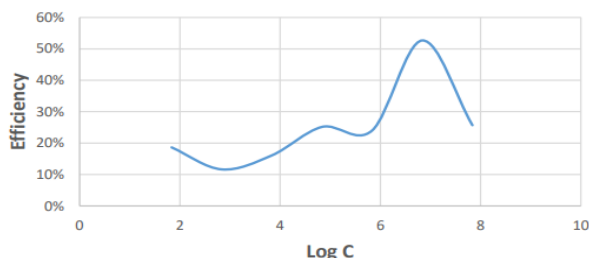
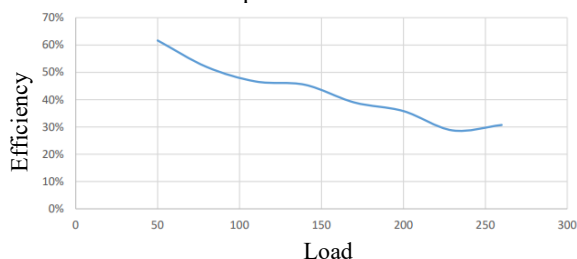a. The capacitance relation.
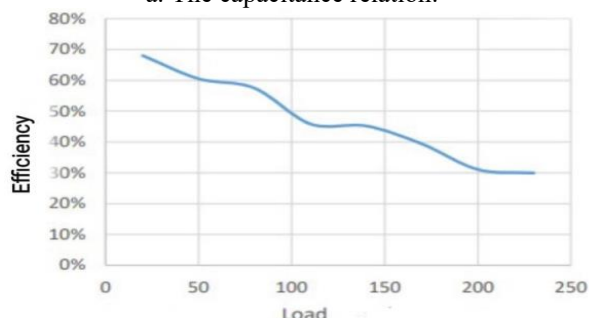
b. The load relation.

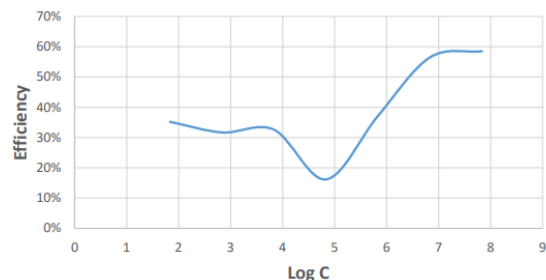Figure 5- Efficiency evaluation at frequency 50 kHz.

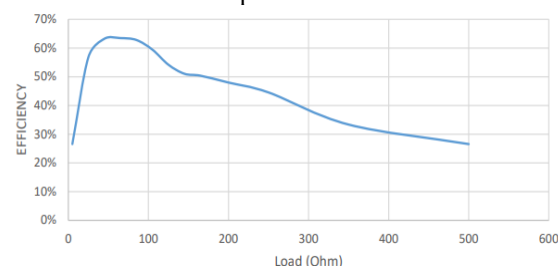a. The capacitance relation.

b. The load relation.

Figure 6- Efficiency evaluation at frequency 60 kHz.

a. The capacitance relation.

b. The load relation.

Figure 7- Efficiency evaluation at frequency 85 kHz.

The abovementioned discussions are related to the assessment of efficiency; however, the efficiency can be high at a low energy-transferring rate. Accordingly, the following discussions present the input and output energy rates to find the highest efficiency at the highest operating power values. Therefore, by evaluating the input power and output power individually and in accordance with the maximum efficiency attained at different frequencies, the corresponding results are recorded in Table (1). From these results, the maximum efficiency can be obtained at the operating frequency of 50 kHz, with the highest output power of 274.5 W. Although the efficiency at the operating frequency of 60 kHz is high, its transferring power is low (185.3 W) compared with the transferring power at 50 kHz.

Table 1- Input and output power of the maximum efficiency at different frequencies.

Frequency (kHz)	Pin (W)	Pout (W)	Efficiency (%)	Voltage (V)	Loading (Ω)
10	53.19	14.36	27.0	400	50
50	403.5	274.5	68.02	400	20
60	280.6	185.3	66.06	400	50
85	318.1	201.8	63.46	400	65

4.2 Available Experimental Implementation
After determining the dimensions of the system and its electrical requirements, the practical step has come by constructing a real system of wireless transferring power. The first step in the experimental implementation is to build a controllable voltage sinusoidal source. It is accomplished using a multi-

level inverter. This inverter circuit is shown in Figure (8), which is a three-cascaded H-bridge producing the 7-level inverter. Each bridge has four IGBT switches with symmetrical supplies.

Hardware simulation is an important process of designing an electronic product using software tools to model and simulate the behavior of a physical hardware system. It involves creating a virtual representation of the hardware system and simulating its behavior under various conditions and scenarios. Hardware simulation can be used to design, test, and optimize a wide range of hardware systems, including electronic circuits, mechanical systems, and control systems. It is particularly useful in the early stages of the design process, where it can help identify design flaws and issues before investing in expensive hardware development. Overall, hardware simulation is a very powerful tool for engineers. In this paper, the Matlab/Simulink program is used to preliminarily test the behavior of the system.

By simulating this inverter in Matlab/Simulink, the simulated control signals that are used as gate pulses are shown in Figure (9.a). They are generated based on the switch status in Table (2). Figure (9.b) shows the simulated voltage and current waveforms of frequency of 85 kHz that ensure the 7 levels and the appropriate current sinewave for a selected inductive load.
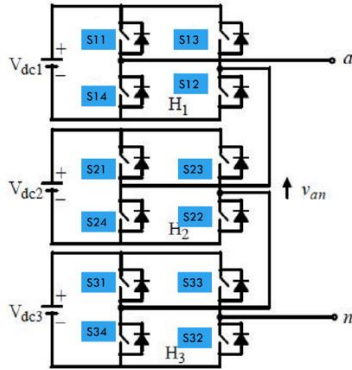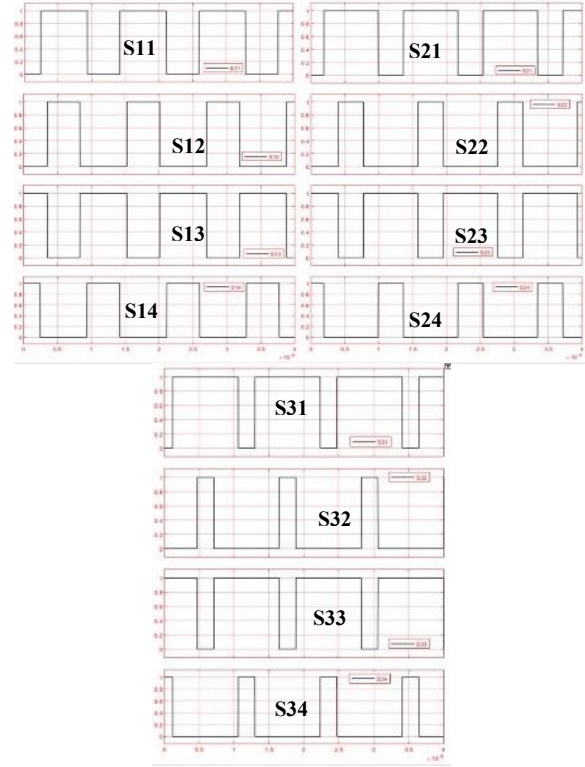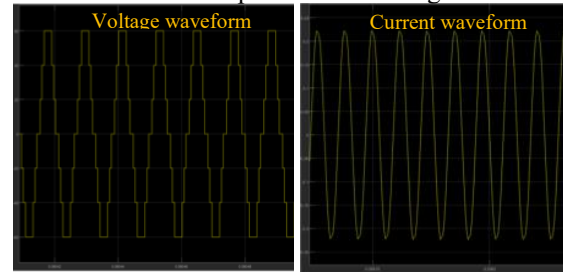

Figure 8- Multi-level inverter circuit (7-level).

Table 2- Truth table of the switches' status of the multilevel voltage (1 is on & 0 is off).

| Level	S11	S12	S13	S14	S21	S22	S23	S24	S31	S32	S33	S34
-3	0	0	1	1	0	0	1	1	0	0	1	1
-2	0	0	1	1	0	0	1	1	1	0	1	0
-1	0	0	1	1	1	0	1	0	1	0	1	0
0	1	0	1	0	1	0	1	0	1	0	1	0
0	1	0	1	0	1	0	1	0	1	0	1	0
1	1	1	0	0	1	0	1	0	1	0	1	0
2	1	1	0	0	1	1	0	0	1	0	1	0
3	1	1	0	0	1	1	0	0	1	1	0	0

a. Gate pulse control using.

b. Simulated waveforms

Figure 9- Matlab/Simulink multi-level inverter.

The simulated control pulses shown in Figure (9) are experimentally generated using the DSP board. The considered DSP board is Raspberry Pi Pico which is a low-cost and high-performance microcontroller board with flexible digital interfaces. Figure (10) shows the generated pulses using the Raspberry Pi Pico. Raspberry Pi Pico is used to pulse the drive circuit with needed high-frequency pulses. However, the generated signals shown in Figure (10) are for the system frequency of 10 kHz due to the experimental limitations. Figure (11) shows the diagram for the power circuit of the multilevel inverter and the design circuit of the drive circuit of the IGBT switch. Of course, it is repeated for each IGBT.

Figure 10- Raspberry Pi Pico DSP board control signals as the output pulses on the switches' gates.

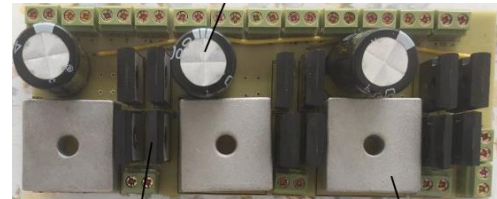a. The diagram of the power circuit of multilevel inverter.
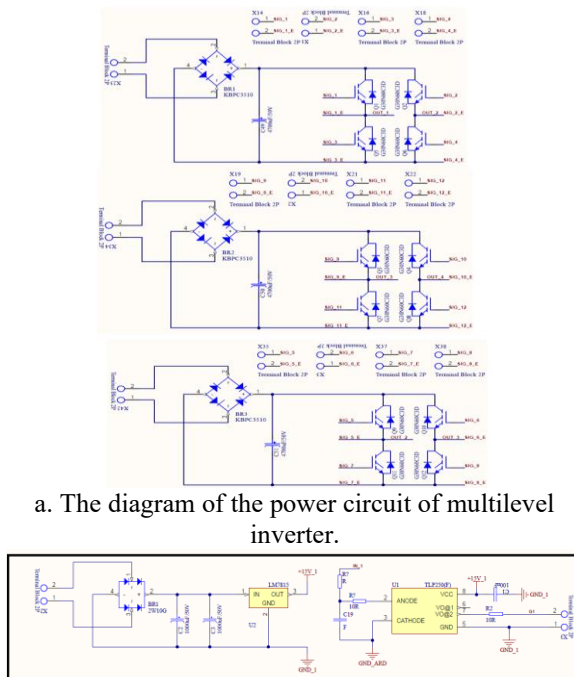
b. Drive circuit for only one switch gate.

Figure 11- The design of the printed diagram.

Figures (12.a) and (12.b) show the implemented drive circuit and the implemented DC power supply circuit, respectively. However, Figure (12.c) shows a complete view of the power electronic circuits to generate the symmetrical DC supplies, the drive circuits of the IGBT, and the required transformers. Figure (12.d) shows the two coils where the lower one is the transmitting coil while the upper one is the receiving coil. All these items and components are
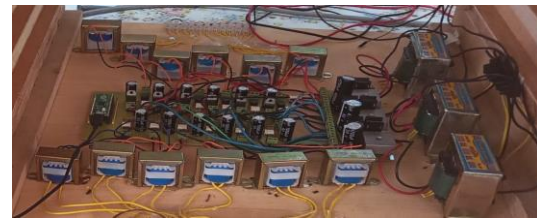
interconnected and controlled using the Raspberry Pi Pico DSP board. However, due to the limitation of the execution time of the utilized DSP board, the system is applied for the 10 kHz frequency for transferring the power utilizing only the three levels of the inverter as shown in Figure (13).
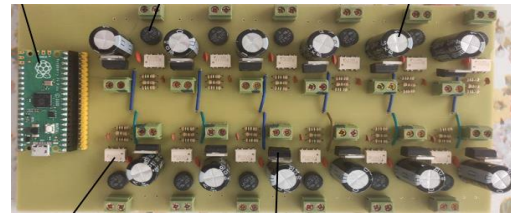
a. Drive Circuit

b. Power circuit.

c. Drive and power circuits for the multilevel inverter.


d. Transmitting and receiving coils.

Figure 12- The design of the printed diagram.

The results shown in Figure (13.a) verify the synchronization of pulses supplying each switch with each corresponding one. The better efficiency of WPT is at a higher frequency, however, the available frequency of 10 kHz for one bridge that specifications give that waveform for voltage of the inverter output as shown in Figure (13.b). Figure (13.c) shows the measured DC voltage at the secondary side for the unloaded system. The current and voltage values were measured at 0.037 A and 12.8 V, respectively at the loading of 34 Ω, where the system frequency is implemented at the 10 kHz. Therefore, the output DC

power is 4.74W. Compared with the mean power on the primary coil, which is found 8.08 W, the efficiency in that case is 58.66%. Comparing practical results with simulated at the same frequency 10 kHz, getting better results in experimental verification because of the effect of magnetic field in coupling. The reason is that there are harmonics at higher frequencies available in the experimental setup that produce further power transferring and therefore improve the coupling.
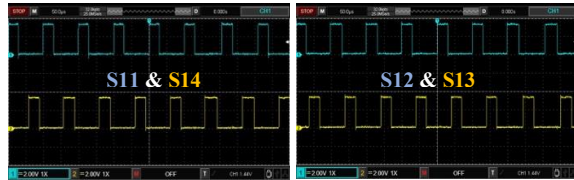
a. The measured gate pulses.
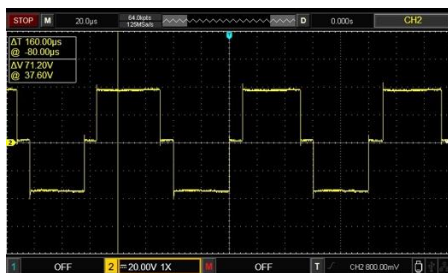
b. The measured inverter voltage waveform.
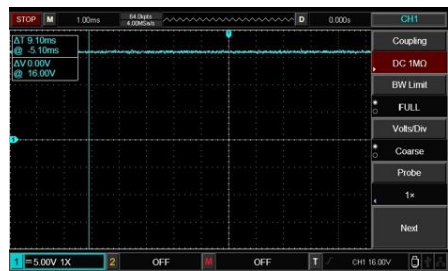
c. The measured output voltage at unload system.

Figure 13- The experimental results.

5. Conclusions

Using EM simulation software -COMSOL-Multiphysics, the axe-symmetric method is unfortunately preferred over the 3D representation because of the execution time limitation of the 3D-based analyses. In this study and concerning the theoretical knowledge, there was a wide range of frequencies to compare and evaluate the power-transferring system efficiencies. Considering the highest efficiency, the best capacitance to reach the system resonance was 1.47 μF. Varying the loads from 20 Ω to 100 Ω on certain frequencies from 5 to100 kHz, the optimum efficiency at 50kHz was 68.02% when the loading resistance was 20 Ω. In that case, the

larger output power was 274.5 W. According to the simulation results, there was a critical point at 50 kHz frequency when the efficiency curve started to decrease. Due to the experimental limitation of implementing high frequency such as 50 kHz, the implemented supply frequency was 10 kHz in the laboratory. A better efficiency was attained using the experimental setup than the simulation results due to the harmonics of high frequencies generated due to the wave chopping created by the inverter to generate the 10 kHz waveform from the DC system. However, in a work to follow, the experimental setup of a power frequency range up to 100 kHz will be desired for accurate performance evaluation of the WPT system.

6. References

[1] W. A. Shah "Analysis and Design of Inductive Power Transfer Systems for Automotive Battery Charging Applications" M.Sc. Thesis in Electrical and Electronic Engineering, The Graduate School of Applied Sciences, Near East University, NICOSIA, the Republic of Cyprus, 2016.

[2] Y. Yao, X. Chen, J. Li, H. Hu, D. Vizzari, Y. Penga "Towards sustainable and efficient inductive charging pavement systems: Current progress and future directions" Construction and Building Materials, 449, 2024.

[3] J. Rahulkumar, R. Narayanamoorthi, R. Vishnuram, C. Balaji, T. Gono, T. Dockal, R. Gono, and P. Krejci "A review on resonant inductive coupling pad design for wireless electric vehicle charging application" Energy Reports, vol. 10, pp. 2047–2079, 2023.

[4] Z. Zhang and H. Pang "Wireless Power Transfer: Principles and Applications", Wiley, 2022

[5] J. L. Villa, J. Sallán, A. Llombart, and J. F. Sanz "Design of a high frequency Inductively Coupled Power Transfer system for electric vehicle battery charge", Applied Energy, 2009.

[6] Y. J. Hwang and J. M. Kim "A Double Helix Flux Pipe-Based Inductive Link for Wireless Charging of Electric Vehicles" World Electric Veh. J. 2020, 11, 33.

[7] D. Kim, A. Abu-Siada, and A. T. Sutinjo "Application of FRA to Improve the Design and Maintenance of Wireless Power Transfer Systems" IEEE Transactions on Instrumentation and Measurement, vol. 68, no. 11, pp. 4313-4325, Nov. 2019.

[8] S. Stoecklin, A. Yousaf, T. Volk, and L. Reindl, "Efficient wireless powering of biomedical sensor systems for multichannel

brain implants**,** IEEE Trans. Instrum. Meas., vol. 65, no. 4, pp. 754–764, Apr. 2016.

[9] V. J. Brusamarello, Y. B. Blauth, R. de Azambuja, I. Müller, and F. R. de Sousa, "Power transfer with an inductive link and wireless tuning," IEEE Trans. Instrum. Meas., vol. 62, no. 5, pp. 924–931**,** May 2013.

[10] A. Triviño-Cabrera, J. M. González-González, and J. A. Aguado "Wireless Power Transfer for Electric Vehicles: Foundations and Design Approach" Power Systems, Springer International Publishing: Cham, Switzerland, 2020; ISBN 978-3-030-26705-6.

[11] T. Bouanou, H. El Fadil, A. Lassioui, O. Assaddiki, S. Njili, "Analysis of Coil Parameters and Comparison of Circular, Rectangular, and Hexagonal Coils Used in WPT System for Electric Vehicle Charging" World Electr. Veh. J. 2021, 12, 45.

[12] T. Bouanou, H. E. Fadil, and A. Lassioui "Analysis and Design of Circular Coil Transformer in a Wireless Power Transfer System for Electric Vehicle Charging Application" In Proceedings of the 2020 International Conference on Electrical and Information Technologies (ICEIT), Rabat, Morocco, 4–7 March 2020; pp. 1–6.

[13] R. Vaka and R. Keshri "Design Considerations for Enhanced Coupling Coefficient and Misalignment Tolerance Using Asymmetrical Circular Coils for WPT System" Arab. J. Sci. Eng. 2019, 44, 1949–1959.

[14] B. Olukotun, J. Partridge, and R. Bucknall "Finite Element Modeling and Analysis of High Power, Low-Loss Flux-Pipe Resonant Coils for Static Bidirectional Wireless" Power Transfer. Energies 2019, 12, 3534.

[15] M. Alsayegh, M. Saifo, M. Clemens, and B. Schmuelling "Magnetic and Thermal Coupled Field Analysis of Wireless Charging Systems for Electric Vehicles" IEEE Trans. Magn., vol. 55, pp. 1–4, 2019

[16] C. Liang, G. Yang, F. Yuan, X. Huang, Y. Sun, and J. Li, K. Song "Modeling and Analysis of Thermal Characteristics of Magnetic Coupler for Wireless Electric Vehicle Charging System" IEEE Access, vol. 8, pp. 173177–173185, 2020.